Optics Communications xxx (2009) xxx–xxx

Contents lists available at ScienceDirect

Optics Communications

journal homepage: www.elsevier.com/locate/optcom

Diode laser spectroscopy of ammonia at 760 nm

A. Lucchesini *, S. Gozzini

Istituto per i Processi Chimico-Fisici (IPCF) – CNR, Area della Ricerca – Via G. Moruzzi, 1 - I-56124 Pisa, Italy

ARTICLE INFO

Article history:
Received 7 April 2009
Received in revised form 22 May 2009
Accepted 24 May 2009
Available online xxxx

PACS:
33.70.Jg
33.20.Kf
07.60.Rd
42.55.Px

Keywords:
Ammonia
Line broadening and shift
Overtone bands
Tunable diode laser

ABSTRACT

A tunable diode laser spectrometer has been employed to examine the unknown overtone absorption lines of NH_3 around 13,100 cm^{-1} (760 nm). The spectrometer sources are commercially available heterostructure AlGaAs tunable diode lasers operating in the "free-running" mode. The detection of the lines has been possible by the use of the wavelength modulation spectroscopy and the second harmonic detection technique. A special algorithm has been used in order to fit the highly modulated absorption lines. The weakest observed resonances have absorption cross sections of the order of $\approx 1 \times 10^{-25}$ cm^2/molecule or ≈ 0.3 km^{-1}/amagat. For some of the more intense lines self-, air-, N_2-, He- and H_2-broadening coefficients have been obtained at room temperature and also some shifting coefficients have been measured.

1. Introduction

In spite of their weakness, overtone and combination tone absorption lines of molecular gases are observable in the visible and in the near infrared part of the e.m. spectrum of the atmosphere of the planets [1], because in that case the optical density is orders of magnitude higher than the one obtainable in the laboratory. NH_3 is present in particular in the atmosphere of Saturn, but it has been observed in the interstellar medium too.

The knowledge of ammonia optical resonances and their behavior with the pressure is important for a better knowledge of the planetary atmospheres themselves. Unfortunately the analysis of ammonia combination overtones ro-vibrational spectra is quite difficult for the many overlapping and interacting bands.

A large number of spectroscopic works that make use of several different techniques [2–7] have been reported so far on ammonia fundamentals and first overtones. Many of them take the advantage of the diode lasers (DLs) as the monochromatic and stable sources giving very interesting results on the line position classification as well as on the collisional broadening and shifting parameters at different temperature.

Here we present a spectroscopic work done at room temperature [$T = (294 \pm 2)$ K], based on the use of not expensive DLs. The frequency modulation (FM) technique here has been utilized to detect and resolve the very weak absorption resonances by taking advantage of the DLs modulability through their injection current. In particular we applied the FM spectroscopy [called "wavelength modulation spectroscopy" (WMS) in cases where the value of the frequency is chosen much lower than the resonance line-width] and the second harmonic detection techniques to the NH_3 optical absorptions around 760 nm belonging presumably to the $3\nu_1 + 2\nu_4$ and $4\nu_3$ overtones.

2. Experimental details

The experimental setup for the absorption spectroscopy by using the WMS and the 2nd harmonic detection has been described in a previous paper [8]. In this work the monochromatic source was a Fabry-Perot type semiconductor diode laser SHARP Mod. LT030MD0, which emits a 3 mW cw at 755 nm at 50 mA without any external optical feedback. This low power was still enough to perform the absorption spectroscopy measurements through the system arranged by the Diode Laser Spectroscopy Laboratory of IPCF-CNR. Thanks to its V-shaped junction cladding layers based on SHARP's original technology (VSIS chip structure) this types of cw diode laser has a single transverse and single longitudinal mode. In the "free-running" configuration adopted here the full width at half the maximum (FWHM) of the DL emission mode is around

* Corresponding author. Fax: +39 0503152 236.
E-mail address: lucchesini@ipcf.cnr.it (A. Lucchesini).

0030-4018/$ - see front matter © 2009 Published by Elsevier B.V.
doi:10.1016/j.optcom.2009.05.049

20 MHz. A confocal 5 cm Fabry–Perot (F.–P.) interferometer was utilized to check the frequency sweep and the laser emission mode. The measurement cell containing the sample gas was a Herriott type multipass, 30 m path length (by S.I.T. s.r.l.: www.scintec.it). Another Herriott cell contained the water vapor for checking whether the obtained absorption features came from H_2O that could contaminate the cell. An iodine reference glass cell was used for the precise wavenumber measurements. For the harmonic detection a sinusoidal current was mixed to the diode laser injection current and then the signal collected by a pre-amplified silicon photodiode was sent to a lock-in amplifier in order to extract the desired harmonic component. The ammonia gas was supplied by Air Liquide: grade N45 (purity 99.995%), $H_2O \leqslant 10$ppmv, $O_2 + Ar \leqslant 2$ppmv, $CO_2 \leqslant 5$ppmv, $CO \leqslant 5$ppmv, $N_2 \leqslant 10$ppmv, and $CH_4 \leqslant 2$ppmv.

2.1. Frequency modulation

In these experiments what has been measured mainly is the transmittance through the gas samples $\tau(\nu)$. This can be described by the Lambert–Beer equation:

$$\tau(\nu) = e^{-\sigma(\nu)z}, \quad (1)$$

where $z = \rho l$ is the product of the absorbing species number density ρ (in molecule/cm^3) and the optical path l (in cm) of the radi-

Table 1
List of the observed NH_3 lines along with the maximum absorption cross sections.

$\nu'(\mathrm{cm}^{-1})$	$\sigma_{max}\left(10^{-24}\frac{\mathrm{cm}^2}{\mathrm{molecule}}\right)$	$\nu'(\mathrm{cm}^{-1})$	$\sigma_{max}\left(10^{-24}\frac{\mathrm{cm}^2}{\mathrm{molecule}}\right)$	$\nu'(\mathrm{cm}^{-1})$	$\sigma_{max}\left(10^{-24}\frac{\mathrm{cm}^2}{\mathrm{molecule}}\right)$
13001.86	0.8 ± 0.1	13049.92	3.9 ± 0.3	13106.71	
13002.85	1.8 ± 0.2	13050.06		13106.84	1.4 ± 0.1
13003.28	6.6 ± 0.5	13050.26		13106.94	
13003.32	6.6 ± 0.5	13068.36	1.7 ± 0.3	13107.15	2.4 ± 0.2
13004.35	1.5 ± 0.2	13068.43		13107.20	
13004.50	2.8 ± 0.1	13068.61		13107.31	2.0 ± 0.1
13011.35	4.1 ± 0.2	13070.78		13107.39	
13011.51	0.9 ± 0.2	13070.85		13107.56	3.2 ± 0.3
13011.61	0.4 ± 0.2	13070.95		13108.11	6.0 ± 0.4
13011.71	1.0 ± 0.2	13071.26	1.1 ± 0.2	13108.17	
13012.09	1.4 ± 0.2	13071.62	4.1 ± 0.3	13109.70	2.6 ± 0.1
13037.42	4.2 ± 0.2	13072.17	2.2 ± 0.2	13114.00	5.9 ± 0.4
13037.61	4.0 ± 0.3	13072.41		13115.77	11.6 ± 0.5
13037.88	2.3 ± 0.4	13072.49	1.5 ± 0.1	13117.46	3.9 ± 0.2
13038.14	1.2 ± 0.3	13072.58	2.2 ± 0.2	13118.24	
13038.40	1.1 ± 0.3	13072.77		13118.30	5.5 ± 0.1
13039.06	3.6 ± 0.3	13072.85		13118.54	0.9 ± 0.1
13039.21	4.5 ± 0.4	13073.08	2.6 ± 0.2	13119.36	4.6 ± 0.2
13039.68	8.1 ± 0.3	13074.66	1.8 ± 0.2	13122.70	1.0 ± 0.1
13039.90	5.7 ± 0.3	13076.22	1.1 ± 0.2	13122.85	1.6 ± 0.1
13040.04	8.0 ± 0.4	13083.81	9.2 ± 0.4	13123.01	1.0 ± 0.1
13040.24		13083.98	0.5 ± 0.1	13126.85	3.2 ± 0.1
13040.34		13104.60		13139.15	1.9 ± 0.2
13040.47		13104.71	1.6 ± 0.1	13139.25	1.6 ± 0.3
13040.57		13106.06	3.1 ± 0.1	13139.91	4.4 ± 0.2
13043.53	2.6 ± 0.2	13106.24	2.8 ± 0.1	13145.94	
13044.10	1.6 ± 0.1	13106.46	0.5 ± 0.1	13146.15	4.9 ± 0.2
13044.45	1.8 ± 0.2	13106.55	0.8 ± 0.1	13146.40	
13149.10	1.6 ± 0.1	13199.91	1.9 ± 0.1	13290.58	0.6 ± 0.1
13152.76		13215.74	0.7 ± 0.1	13291.35	1.3.±0.1
13152.90	2.4 ± 0.2	13218.59	1.4 ± 0.1	13291.90	
13155.68	3.9 ± 0.2	13218.91	1.6 ± 0.1	13291.99	
13157.39	3.0 ± 0.1	13225.04	1.4 ± 0.1	13292.10	
13158.24		13233.10	2.9 ± 0.1	13292.21	
13158.34		13233.74	2.0 ± 0.1	13292.33	
13161.87	1.1 ± 0.1	13234.12	0.4 ± 0.1	13292.42	0.1 ± 0.1
13171.14	2.6 ± 0.2	13237.37	0.8 ± 0.1	13292.56	
13172.30	3.4 ± 0.1	13237.73	1.5 ± 0.1	13292.66	0.2 ± 0.1
13172.56	3.9 ± 0.1	13239.61	1.7 ± 0.1	13293.25	0.2 ± 0.1
13173.34	4.9 ± 0.2	13240.34	2.0 ± 0.1	13293.44	0.3 ± 0.1
13173.61	1.4 ± 0.1	13240.38		13295.41	0.2 ± 0.1
13173.98	3.8 ± 0.2	13240.47	1.5 ± 0.1	13297.24	0.3 ± 0.1
13175.35	1.1 ± 0.1	13240.56	1.5 ± 0.1	13306.72	0.7 ± 0.1
13175.44		13242.36	1.1 ± 0.1	13306.86	1.1 ± 0.1
13178.01	0.8 ± 0.1	13246.47	1.1 ± 0.1	13311.75	1.1 ± 0.3
13178.72	1.5 ± 0.2	13243.56		13312.24	
13183.95	4.5 ± 0.1	13246.73	0.6 ± 0.1	13314.94	0.3 ± 0.2
13184.07		13246.84	0.6 ± 0.1	13315.57	0.4 ± 0.2
13184.45	0.6 ± 0.1	13248.52	0.9 ± 0.2	13330.52	0.7 ± 0.1
13196.13	0.9 ± 0.1	13248.90	0.9 ± 0.2	13337.28	0.4 ± 0.1
13196.32	0.6 ± 0.1	13252.54	0.3 ± 0.1	13337.46	
13196.63	0.5 ± 0.1	13259.95	1.6 ± 0.1	13339.90	1.5 ± 0.1
13196.76	0.6 ± 0.1	13267.85	0.6 ± 0.1	13344.68	1.3 ± 0.1
13197.53	3.1 ± 0.1	13268.26	0.3 ± 0.1	13346.05	0.3 ± 0.1
13197.70	1.1 ± 0.1	13268.44	0.6 ± 0.1	13354.53	0.2 ± 0.1
13197.93	2.5 ± 0.1	13275.31	1.2 ± 0.1	13354.87	0.3 ± 0.1
13198.16	1.8 ± 0.1	13287.42	0.4 ± 0.1	13363.22	0.5 ± 0.3
13198.73	3.0 ± 0.2	13289.16	1.9 ± 0.1		

Please cite this article in press as: A. Lucchesini, S. Gozzini, Opt. Commun. (2009), doi:10.1016/j.optcom.2009.05.049

ation through the sample, i.e. the column amount (in molecule/cm^2); the absorption cross section $\sigma(\nu)$ is therefore expressed in cm^2/molecule. If $\sigma(\nu)z \ll 1$, that is in the small optical depth regime, as in our case, Eq. (1) can be approximated:

$$\tau(\nu) \simeq 1 - \sigma(\nu)z. \tag{2}$$

where $\sigma(\nu)$ must behave as the shape of the absorption line: Gaussian-like for the Doppler broadening and Lorentzian-like for the collisional broadening. Other effects, like the Dicke narrowing that occurs when the molecular mean free path is comparable to the wavelength of the radiation [9], are not observed in our measurement conditions, at least within our sensitivity, and are not taken into account.

The Voigt function, a convolution of the Lorentz and the Gauss curves, describes the behavior of the optical absorption as a function of the radiation frequency:

$$f(\nu) = \int_{-\infty}^{+\infty} \frac{\exp[-(t-\nu_\circ)^2/\Gamma_G^2 \ln 2]}{(t-\nu)^2 + \Gamma_L^2} dt, \tag{3}$$

where $\nu_\circ$ is the gas resonance frequency, Γ_G and Γ_L are the Gaussian and the Lorentzian half-widths at half the maximum (HWHM) respectively.

We used the FM technique and therefore the emission frequency of the source $\bar{\nu}$ was sinusoidally modulated at the frequency $\nu_m = \omega_m/2\pi$ resulting in

$$\nu = \bar{\nu} + a\cos\omega_m t. \tag{4}$$

In this case the transmitted intensity depends on both the line shape and the modulation parameters, and can be written as a cosine Fourier series:

$$\tau(\bar{\nu} + a\cos\omega_m t) = \sum_{n=0}^{\infty} H_n(\bar{\nu}, a)\cos n\omega_m t, \tag{5}$$

where $H_n(\bar{\nu})$ is the n-th harmonic component of the modulated signal. By using a lock-in amplifier tuned to a multiple $n\nu_m (n = 1, 2, \ldots)$ of the modulation frequency, the output signal is proportional to the n-th component $H_n(\bar{\nu})$ and when the amplitude a is chosen smaller than the width of the line, the n-th Fourier component is proportional to the n -order derivative of the original signal:

$$H_n(\bar{\nu}, a) = \frac{2^{1-n}}{n!} a^n \frac{d^n \tau(\nu)}{d\nu^n}|_{\nu=\bar{\nu}}, \quad n \geqslant 1. \tag{6}$$

For the pressure broadening and shift measurements performed in this work a low modulation amplitude has been used and the second harmonic component detected ($2f$ detection), therefore the output signal was proportional to the second order derivative of the real absorption line. This expedient not only enhanced the signal-to-noise (S/N) ratio, but also reduced to zero the unwanted background. Then a nonlinear least-squares fit procedure explained elsewhere [10] has been used in order to extract the line parameters. In particular we interpreted the Lorentzian FWHM γ_L, the collisional component of the line-shape, as a function of the total pressure p by the general expression:

$$\gamma_L(p) = 2\Gamma_L(p) = \gamma_i p_i + \gamma_{self} p_\circ, \tag{7}$$

where $p_\circ$ is the partial pressure of the studied gas, p_i is partial pressure of the buffer gas i, γ_i is the FWHM broadening coefficient related to the buffer gas, and γ_{self} is the sample gas FWHM self-broadening coefficient.

To obtain the line positions even for the weakest lines we have also been obliged to use large values of the modulation amplitude parameter m ($m = a/\Gamma = 2.2 - 2.3$ typically). This substantially improved the S/N ratio, but did not permit the utilization of Eq. (6) any more. The approximated function that well describes the absorption line distorted by modulation has been appositely calculated and it is reported in the Appendix.

3. Experimental results

At 760 nm a very few absorption measurements on gaseous ammonia have been found in the literature. The presence of a weak absorption band in this region have been noticed in the atmosphere of Jupiter [11] with absorption coefficients similar to ours, and also by a spectroscopic work in the laboratory [12], but no systematic measurements have been carried on so far.

By the WMS technique we observed 173 ammonia absorption lines and we could measure the maximum absorption cross sections of most of them, all obtained at the same values of pressure ($p \simeq 30$ Torr) and temperature (RT). The results are in Table 1. Their positions are reported with 0.01 cm^{-1} maximum error (3σ). For the 13049.92, 13050.06, 13050.26, 13145.94, 13146.15 and 13146.40 cm^{-1} lines, instead of I_2, water vapor have been used as the reference [13], because it was impossible to find close I_2 lines having enough strengths to be well detected. For some of the most intense lines for which the error was acceptable, we integrated the absorption coefficient in energy in order to obtain the line strength (S), and the results are shown in Table 2.

By following the intensity distribution it can be said that the $3\nu_1 + 2\nu_4$ combination overtone band presumably arrives to 13250 cm^{-1} and beyond there should be the $4\nu_3$ band, as it can be deduced from [14] and [15]. Because of the complexity of the structure of the overtone band it is not possible to give a specific quantum classification of the ro-vibrational transitions. In fact for these highly excited levels the numerous possible resonances between the levels can modify significantly the intensity and the position of the expected lines [16]. An aid to the classification job could come from working at very low temperature ($\leqslant 20$ K) by using the supersonic jet expansion [17,18]. In this case only a few first rotational levels will be populated and the level superpositions will be smaller or absent. Hopefully this will be one of our future projects.

In Fig. 1 the ammonia 13037.42, 13037.61, 13037.88, 13038.14 and 13038.40 cm^{-1} lines are shown (a) as obtained by WMS and 2nd harmonic detection, while the F.–P. transmission signal (b) is contemporary collected in order to check the frequency sweep amount. In the background a small etalon effect is present, originated by the many reflections inside the measurement cell and by the non perfect collimation of the laser beam. The DL mode intensity change directly connected to the photon energy (frequency) variation is evident in (b).

3.1. Ammonia line broadening and shifting measurements

Pressure broadening coefficients for ammonia by it-self, and by air, N_2, H_2 and He gases at RT have been measured for some of the

Table 2
Ammonia absorption line strengths.

ν'(cm^{-1})	$S\left(10^{-26}\frac{\text{cm}}{\text{molecule}}\right)$
13039.68	5.7 ± 0.2
13083.81	6.0 ± 0.3
13114.00	3.4 ± 0.2
13115.77	7.7 ± 0.3
13117.46	2.4 ± 0.1
13139.91	4.2 ± 0.2
13157.39	2.2 ± 0.1
13171.14	1.8 ± 0.1
13173.34	3.8 ± 0.2
13173.98	2.5 ± 0.1
13178.72	1.0 ± 0.1
13289.16	1.3 ± 0.1

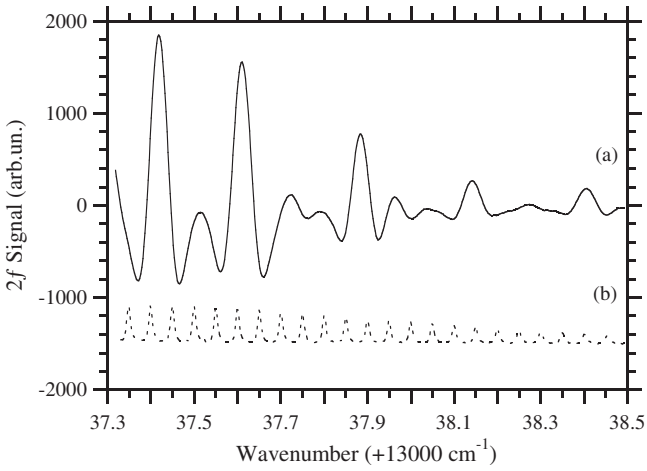

Fig. 1. Second derivative signal of the ammonia spectrum around 766.8 nm (a) obtained by WMS with 10 Hz bandwidth at $p_{NH_3} = 19$ Torr and $T = 294$ K. The F.–P. transmission signal (b) is shown dotted.

more intense and well isolated lines, and the pressure shift coefficients have been obtained for the 13157.39 cm^{-1}. They are shown in Tables 3 and 4, respectively. During the foreign gas broadening measurements the ammonia pressure was kept around 20 Torr, while the host gas partial pressures ranged between 10 and 150 Torr. It can be verified there that ammonia dipole moment makes the self-broadening coefficients much larger than the ones coming from non-dipolar perturbers. In Table 3 the strange abnormal values of He-broadening coefficients at 13139.91 cm^{-1} suggests that perhaps this is not a single line. For the 13171.14 and 13178.72 cm^{-1} lines only the self-broadening coefficients could be collected, because the foreign gas broadening measurements had not enough S/N ratios to give reliable results. It was also impossible to measure the air-broadening coefficient of the 13114.00 cm^{-1} line for the presence of a very close O_2 line (13114.10 cm^{-1}) that interfered.

In some cases of the He- and H_2-broadening experiments, the ammonia sticking effect on the measurement cell wall was evidenced from a non-linear behavior of the FWHM when increasing the host gas pressure, particularly at low pressure. This is a well known effect [19] that can be reduced by choosing the appropriate coating of the cell walls. In our case this was not possible and it was also impossible to increase the cell temperature to avoid ammonia condensation. We limited ourselves to remove the first few measurements points that were clearly out of the expected linear behavior with the pressure.

An example of the ammonia self-broadening and shift measurements at RT are reported in Fig. 2 for the 13157.39 cm^{-1} line.

Table 4
Ammonia pressure shift coefficients (δ).

$\nu'(cm^{-1})$	δ_{self} (MHz/Torr)	δ_{N_2} (MHz/Torr)	δ_{H_2} (MHz/Torr)	δ_{He} (MHz/Torr)
13157.39	−0.8 ± 0.4	0.4 ± 0.2	0.4 ± 0.4	0.9 ± 0.4

We did not find any broadening and shift measurements in the literature on this same band, therefore a comparison can be done only with the fundamentals and first overtones, for which instead many papers can be found.

On the ν_1 fundamental Pine et al. [20] obtained self-, N_2- and H_2-broadening coefficients that in average are on the same order of magnitude than ours, but our He-broadenings are systematically higher. On the ν_2 and the ν_4 fundamentals Baldacchini and colleagues [21–23] calculated and measured the self-broadening and shift coefficients. Their results are similar to ours with the exception of the He-broadenings on the aQ(9,9) line at 921.2550 cm^{-1} of the ν_2 band, where their coefficients are lower than ours. In the work by Bouanich and coworkers [24,25] again on the ν_2 and the ν_4 the self- and He-broadening values, in average, are not far from ours. Measurements and calculations on pressure broadening of ammonia have been carried on also by Dhib and coworkers [26] on the ν_4 band. With helium as the host gas their results are little higher than ours. In the ν_2 band Dhib et al. [27] obtained N_2- and air-broadening coefficients little lower than or equal to ours. In the ν_4 band Hadded et al. [28] measured and calculated the self-, He-, H_2- and Ar-broadening coefficients. In comparison our coefficients are similar with the exception of the He-broadenings that in our case are higher. Later on in the ν_4 and $2\nu_2$ bands Nouri et al. [29] measured N_2- and H_2-broadening coefficients and their results are again comparable to ours. In the $\nu_1 + \nu_3$ band Cubillas et al. [7] obtained in average self-broadenings similar to ours. In the same combination band Kosheley et al. [5] measured the N_2-broadening coefficients at 297 K, and in average their results comes to be little lower than ours. Some lines in the $\nu_1 + \nu_3$ band have been studied also by Gibb et al. [30] and the N_2- and H_2 -broadening coefficients at 294 K are a little lower than ours: they fitted the resonances by the Galatry function [31] as they observed the Dicke narrowing effect. Between 6850 and 7000cm^{-1} air- and N_2-broadening coefficients have been measured by O'Learly et al. [6] and in average they are similar to ours, while the self-broadening coefficients are considerably higher.

For what the ammonia shifting measurements concerns, yet there are no results for the absorption band faced in this work. In any case our few data are comparable to what found in the literature for the N_2-shift [27] and for the self-shift [23] on the ν_2 band, and for the H_2-shift [32,27] on the ν_4 and $2\nu_2$ bands. A big difference has to be reported for the line-shift by He on the ν_4 band, where Dhib and coworkers [33] found almost always negative shift

Table 3
Ammonia pressure broadening FWHM coefficients (γ).

$\nu'(cm^{-1})$	γ_{self} (MHz/Torr)	γ_{air} (MHz/Torr)	γ_{N_2} (MHz/Torr)	γ_{H_2} (MHz/Torr)	γ_{He} (MHz/Torr)
13039.68	52 ± 2	10.3 ± 0.1	11 ± 1	9.1 ± 0.7	6 ± 1
13083.81	41.5 ± 0.7	9 ± 1	7.2 ± 0.7	8.9 ± 0.4	4.8 ± 0.6
13114.00	23.6 ± 0.3	8.6 ± 0.5	6.6 ± 0.5	4.0 ± 0.6	
13115.77	27.0 ± 0.2	7.5 ± 0.3	9.1 ± 0.6	7.3 ± 0.4	3.7 ± 0.3
13117.46	29 ± 1	11 ± 2	10 ± 1	13 ± 2	5 ± 2
13139.91	45 ± 2	9.0 ± 0.6	11.1 ± 0.9	7 ± 1	14.5 ± 0.6
13157.39	24.6 ± 0.4	12.5 ± 0.2	10.1 ± 0.5	10.3 ± 0.4	5.8 ± 0.4
13171.14	28 ± 1				
13173.34	27.6 ± 0.4	9 ± 1	10 ± 1	8.4 ± 0.6	4.3 ± 0.5
13173.98	21.3 ± 0.8	6 ± 1	8 ± 2	7 ± 2	5 ± 1
13178.72	28 ± 2				
13289.16	20.5 ± 0.2	8 ± 1	9.7 ± 0.5	9.5 ± 0.7	4 ± 1

Please cite this article in press as: A. Lucchesini, S. Gozzini, Opt. Commun. (2009), doi:10.1016/j.optcom.2009.05.049

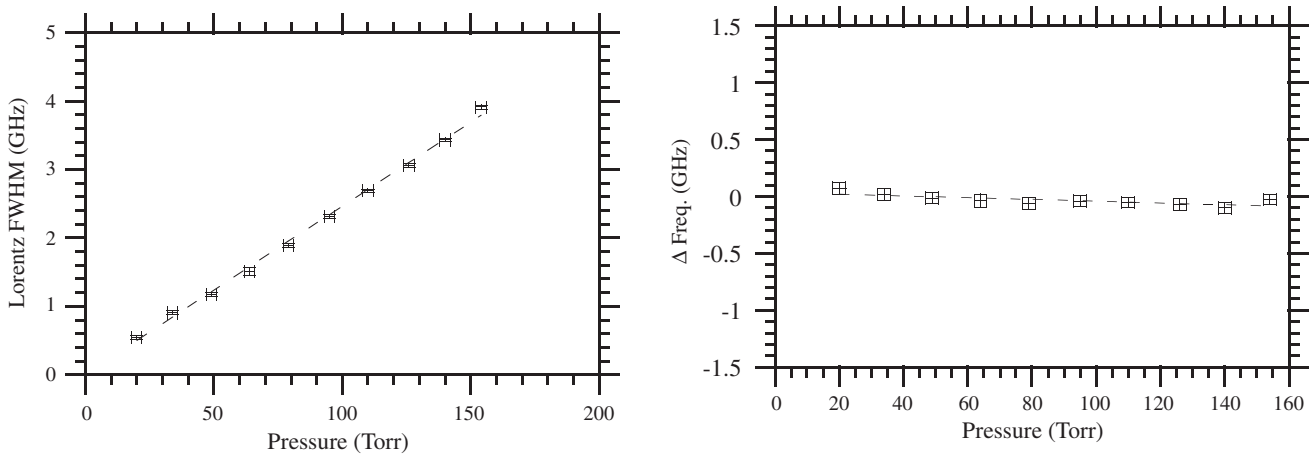

Fig. 2. Self-broadening (left) and self-shift (right) measurements for the 13157.39 cm^{-1} ammonia absorption line as a function of the pressure at room temperature.

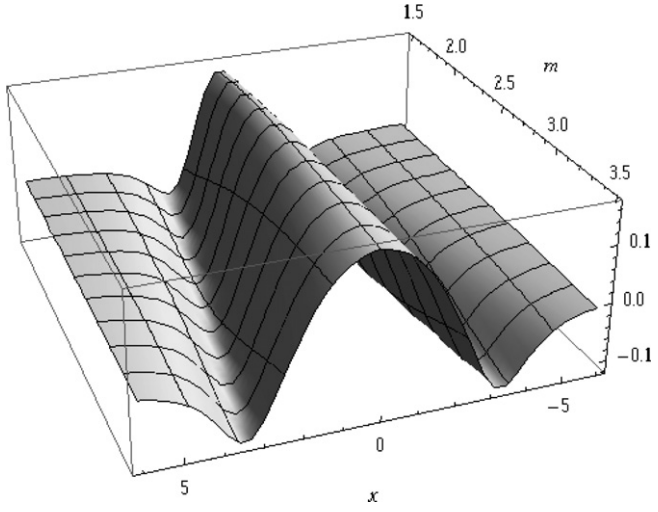

Fig. 3. Behavior of Eq. (13) as a function of the modulation parameter m.

coefficients, but this can be explained by the strong dependence of this effect on the vibrational state, as they mention in their work.

4. Conclusion

By using a tunable diode laser spectrometer with high resolving power ($\lambda/\Delta\lambda \approx 10^7$), the aid of the wavelength modulation spectroscopy technique with the second harmonic detection, and a 30 m total path-length multipass measurement cell, 173 NH_3 lines around 13,100 cm^{-1}, and their positions have been measured within 0.01 $cm^{-1}(3\sigma)$. The ammonia lines presumably constitute the $3\nu_1 + 2\nu_4$ and the $4\nu_3$ combination overtone bands. The line positions have been obtained by the comparison with reference I_2 absorptions and the utilization of a very precise atlas. When using a high modulation index, a properly suited function has been used in order to fit the distorted absorption lines. The maximum absorption cross section of the observed lines are in the 10^{-25}–10^{-24} cm^2/molecule ranges at room temperature. The corresponding strengths are in the 10^{-26} cm/molecule order of magnitude. The collisional broadening coefficients for different perturbing gases have been measured at room temperature for some of the more intense lines and the collisional shifting has been measured for one line. A comparison with the results found in the literature at different wavelengths is reported.

Acknowledgements

The authors wish to thank Dr. D. Bertolini for the calculations in the high modulation approximation, Mr. R. Ripoli for the mechanical set up and Mr. Mauro Tagliaferri for the technical assistance.

Appendix A. Frequency modulation in the high amplitude regime

When the modulation amplitude a is increased, the derivative approximation of Eq. (6) fails and the nth harmonic component $H_n(\nu, a)$ becomes [34]

$$H_n(\nu, a) = \frac{2}{\pi}\int_0^{\pi} \tau(\nu + a\cos\theta)\cos n\theta \, d\theta. \tag{8}$$

The analytical evaluation of this integral is not always possible. Arndt [35] and Wahlquist [36] derived the analytical form of the harmonic components for a Lorentzian function, valid for the collisional component of the absorption line-shape. The expression for the nth harmonic component can be obtained by inverting Eq. (5):

$$H_n(x, m) = \varepsilon_n \mathrm{i}^n \int_{-\infty}^{+\infty} \hat{\tau}(\omega) J_n(m\omega) e^{\mathrm{i}\omega x} d\omega, \tag{9}$$

where

$$\hat{\tau}(\omega) = \frac{1}{2\pi}\int \tau(x) e^{-\mathrm{i}\omega x} dx \tag{10}$$

is the Fourier transform of the transmittance profile; $x = \nu/\Gamma$ and $m = a/\Gamma$ are respectively the frequency and the amplitude of the modulation, normalized to the line-width Γ; J_n is the nth order Bessel function; $\varepsilon_0 = 1, \varepsilon_n = 2 (n = 1, 2, \ldots)$ and i is the imaginary unit. Assuming a Lorentzian absorption line-shape centered at $\nu = 0$ (this is acceptable when, as in this case, collisional broadening dominates) the cross-section coefficient will be

$$\sigma_L(x, m) \propto \frac{1}{1 + (x + m\cos\omega t)^2}. \tag{11}$$

Referring to the work of Arndt we recalculated the second Fourier component of the cross-section coefficient by putting $n = 2$:

$$H_2(x, m) = -\frac{1}{m^2}\left[\frac{\{[(1 - \mathrm{i}x)^2 + m^2]^{1/2} - (1 - \mathrm{i}x)\}^2}{[(1 - \mathrm{i}x)^2 + m^2]^{1/2}} + \text{c.c.}\right] \tag{12}$$

and by eliminating the imaginary part:

$$H_2(x,m) = \frac{2}{m^2} - \frac{2^{1/2}}{m^2} \times \frac{1/2[(M^2+4x^2)^{1/2}+1-x^2][(M^2+4x^2)^{1/2}+M]^{1/2}+|x|[(M^2+4x^2)^{1/2}-M]^{1/2}}{(M^2+4x^2)^{1/2}}, \quad (13)$$

where

$$M = 1 - x^2 + m^2.$$

The behavior of Eq. (13), which is proportional to the 2nd derivative of the absorption feature only for low modulation, is shown in Fig. 3 as a function of the modulation parameter m. For $m = 3$ the 2nd derivative is completely deformed by broadening, as it happens in the reality.

References

[1] E. Karkoschka, Icarus 97 (1992) 161.
[2] S.L. Coy, K.K. Lehmann, J. Chem. Phys. 84 (1986) 5239.
[3] H. Aroui, M. Broquier, A. Picard-Bersellini, J.-P. Bouanich, M. Chevalier, S. Gherissi, J. Quant. Spectrosc. Radiat. Trasfer 60 (1998) 1011.
[4] R. Engeln, G. Berden, R. Peeters, G. Meijer, Rev. Sci. Instrum. 69 (1998) 3763.
[5] M.A. Kosheley, M.Y. Tretyakov, R.M. Lees, L.-H. Xu, Appl. Phys. B 85 (2006) 273.
[6] D.M. O'Leary, J. Orphal, A.A. Ruth, U. Heitmann, P. Chelin, C.E. Fellows, J. Quant. Spectrosc. Radiat. Transfer 109 (2008) 1004.
[7] A.M. Cubillas, J. Hald, J.C. Petersen, Opt. Express 16 (2008) 3976.
[8] A. Lucchesini, S. Gozzini, J. Quant. Spectrosc. Radiat. Transfer 103 (2007) 209.
[9] R.H. Dicke, Phys. Rev. 89 (1953) 472.
[10] M. De Rosa, A. Ciucci, D. Pelliccia, C. Gabbanini, S. Gozzini, A. Lucchesini, Opt. Commun. 147 (1998) 55.
[11] N. Bowles, S. Calcutt, P. Irwin, J. Temple, Icarus 196 (2008) 612.
[12] K.K. Lehmann, S.L. Coy, private communication.
[13] L.S. Rothman et al., J. Quant. Spectrosc. Radiat. Transfer 96 (2005) 139.
[14] G. Herzberg, Infrared and Raman Spectra of Polyatomic Molecules, D. Van Nostrand Co., Princeton, NJ, 1945.
[15] J.O.P. McBride, R.W. Nicholls, J. Phys. B 5 (1972) 408.
[16] L. Halonen, J. Chem. Phys. 106 (1997) 831.
[17] A. Campargue, D. Permogorov, R. Jost, J. Chem. Phys. 102 (1995) 5910.
[18] M. Hippler, M. Quack, Chem. Phys. Lett. 314 (1999) 273.
[19] G. Baldacchini, A. Bellatreccia, F. D'Amato, ENEA Report RT/INN/93/07, 1993.
[20] A.S. Pine, V.N. Markov, J. Mol. Spectrosc. 228 (2004) 121.
[21] G. Baldacchini, G. Buffa, F. D'Amato, O. Tarrini, M. De Rosa, F. Pelagalli, J. Quant. Spectros. Radiat. Transfer 67 (2000) 365.
[22] G. Baldacchini, G. Buffa, O. Tarrini, Nuovo Cimento D 13 (1991) 719.
[23] G. Baldacchini, F. D'Amato, G. Buffa, O. Tarrini, M. De Rosa, F. Pelagalli, J. Quant. Spectrosc. Radiat. Transfer 68 (2001) 625.
[24] J.-P. Bouanich, H. Aroui, S. Nouri, A. Picard-Bersellini, J. Mol. Spectrosc. 206 (2001) 104.
[25] H. Aroui, S. Nouri, J.-P. Bouanich, J. Mol. Spectrosc. 220 (2003) 248.
[26] M. Dhib, J.-P. Bouanich, H. Aroui, M. Broquier, J. Mol. Spectrosc. 202 (2000) 83.
[27] M. Dhib, N. Ibrahim, P. Chelin, M.A. Echargui, H. Aroui, J. Orphal, J. Mol. Spectrosc. 242 (2007) 83.
[28] S.Haddedd.H. Aroui, J. Orphal, J.-P. Bouanich, J.-M. Hartmann, J. Mol. Spectrosc. 210 (2001) 275.
[29] S. Nouri, J. Orphal, H. Aroui, J.-M. Hartmann, J. Mol. Spectrosc. 227 (2004) 60.
[30] J.S. Gibb, G. Hancock, R. Peverall, G.A.D. Ritchie, L.J. Russell, Eur. Phys. J. D 28 (2004) 59.
[31] L. Galatry, Phys. Rev. 122 (1961) 1218.
[32] M. Dhib, M.A. Echargui, H. Aroui, J. Orphal, J.-M. Hartmann, J. Mol. Spectrosc. 233 (2005) 138.
[33] M. Dhib, M.A. Echargui, H. Aroui, J. Orphal, J. Mol. Spectrosc. 238 (2006) 168.
[34] C.R. Webster, R.T. Menzies, E.D. Hinkley, Laser Remote Chemical Analysis, Wiley, New York, 1988. p. 215.
[35] R. Arndt, J. Appl. Phys. 36 (1965) 2522.
[36] H. Wahlquist, J. Chem. Phys. B 35 (1961) 1708.